Lung Bioaccessibility of Manganese in Arc Welding Fume

Christopher Warner

A thesis
submitted in partial fulfillment of the
requirements for the degree of

Master of Science

University of Washington
2014

Committee:
Noah Seixas
Michael Morgan
Christopher Simpson

Program Authorized to Offer Degree:
Environmental and Occupational Exposure Science

University of Washington

Abstract

Lung Bioaccessibility of Manganese in Arc Welding Fume

Christopher Warner

Chair of the Supervisory Committee:
Professor Noah Seixas
Department of Environmental & Occupational Health Sciences

Workers chronically exposed to manganese (Mn) are at increased risk for the development of a Parkinsonism syndrome called manganism. A longitudinal cohort study worked with students at a welding training school to investigate the viability of using Mn levels in various biological compartments to indicate exposure to Mn, which is a component of welding fume. Associations between airborne Mn exposure and Mn concentrations in the body were unclear. It is hypothesized that elucidation of the site of deposition of the fume particles in the respiratory tract and the degree to which the deposited particles dissolve may help to explain the lack of a stronger relationship. Mn in welding fume exists as part of complex particles, from which it must dissolve in order to pass from the lungs into the blood. Solubility depends on the physical characteristics of the particles, but is also a function of the location in the respiratory tract in which they are deposited. That location, in turn, is largely a function of particle size. Thus, to improve estimates of the potential systemic dose of Mn from welding fume, we measured

particle size distributions and the solubility of Mn in fume from five types of welding (SMAW, GMAW, FCAW-dual shield, and FCAW-inner shield, and GTAW). Particle size distributions were measured by gravimetric analysis of PTFE substrates used in a 10 stage Micro-Orifice Uniform Deposit Impactor. Fume was collected for solubility tests on MCE filters. The filters were leached at 37 C in a simulated alveolar lining fluid (Hatch's solution) for 1, 24, 48, or 96 hours. Following separation of soluble Mn with a centrifugal filtering device, the dissolution of the Mn from the particles was calculated by comparing, with inductively-coupled plasma mass spectrometry, the Mn content of the solution and of the remaining filter. Mass median aerodynamic diameters (MMAD) were not statistically different between methods of welding. Average MMADs for each type ranged from 0.88 µm to 1.25 µm. Geometric standard deviations (GSD) averaged between 3.5 and 4 for all welding methods except GTAW, for which average GSD was 6.21. All five welding methods showed a tendency toward a bimodal distribution, with one mode near 0.4 µm, and a less pronounced mode in the range of 2-5 µm. A model of respiratory deposition indicated that approximately 5.7% of the mass of fume in the samples would deposit in the alveolar region. The average percent of Mn that dissolved in Hatch's solution for all samples was 3.21. A clear trend in dissolution with respect to leaching duration was seen only in the fume from GTAW, for which the percent of total Mn dissolved decreased with leaching duration. Deposition estimates and solubility together indicate that only approximately 0.2% of the Mn in inhaled welding fume will become available for uptake into the blood.

Background

Manganese (Mn) is a trace metal essential for development and function throughout the body. Most people ingest sufficient amounts from common foods; deficiency is rare and excess is quickly excreted (Aschner and Aschner, 2005). Overexposure, which is possible from inhalation of airborne Mn, increases the risk of central nervous system impairment, including slowed reaction time, sleep disturbance, and tremor (Ellingsen et al., 2008, Sjogren et al., 1996, Bowler et al., 2007). Excessive inhaled Mn is rare outside of occupational settings, but is a concern in certain industries, such as Mn mining, ore refining, and in welding, which generates fume containing Mn (ATSDR, 2012). Manganism, a syndrome attributable to excessive Mn inhalation, has many symptoms similar to those of Parkinson's disease (ATSDR, 2012).

Of interest for occupational monitoring and for epidemiological exposure assessment is a biomarker that could be used to accurately estimate Mn exposure. Several studies have explored the usefulness of blood Mn content for this purpose. Blood Mn was useful for discrimination between exposed and unexposed groups of Mn alloy producers (Apostoli et al., 2000) and Mn oxide manufacturers (Roels et al., 1987) but was not accurate enough for use as an individual biomarker. Among welders, Ellingsen, et al. (2006) also found that, while group mean blood Mn concentrations were different between welders and referents, the ranges of individual concentrations from both groups widely overlapped. From 2011 to 2014 we conducted a study with a cohort of welding students at a technical college, comparing Mn in whole blood to exposure to airborne Mn in welding fume. We also found the relation between airborne Mn exposure and blood Mn to be unclear. We hypothesize that characterizing two aspects of welding fume, the site of its deposition in the respiratory tract and the degree to which Mn contained in it

dissolves in lung fluid, may improve the accuracy of welding fume exposure as a measure of Mn dose.

Mn is a crucial component of welding materials. It is present in various amounts in consumable rods and wire, and in stainless and mild steel as an alloy increase the strength and workability of the metal. It becomes a part of welding fume, of which it makes up 0.2-10% by weight, when the intense heat of the welding arc vaporizes metal (Taube, 2013). Within fractions of a second of vaporization, the metal cools, condenses, and begins to aggregate with other particles while also undergoing reactions with other vaporized metals, shielding gases, flux components, and surrounding air (Vishnyakov et al., 2013, Berlinger et al., 2011). As a result, Mn is present in numerous compounds in welding fume. Most common are oxides such as MnO_2, MnO, and Mn_3O_4, but silicates, fluorides, and mixed-metal oxides, such as $MnFe_2O_4$, are also present (Taube, 2013).

Welding fume is a complex aerosol with particles ranging in size from ultrafine (less than 0.1 µm in diameter) to approximately 20 µm in diameter (Oprya et al., 2012). It consists of primary particles of around 5-40 nm in diameter and larger, chain-like, agglomerated particles (Berlinger et al., 2011). Nearly all particles, including agglomerates, are in the respirable size range. The majority of mass is in particles with aerodynamic diameters between 0.1 – 1.0 µm (Hewett, 1995b). A particle's aerodynamic diameter is the diameter of a hypothetical spherical particle of density 1 g/cm^3 that behaves in the same way in an airstream. For example, a particle might be 2 µm long and 0.1 µm wide, but if it settles out of an airstream at the same velocity as a 0.3 µm-diameter sphere of the same density, its aerodynamic diameter would be 0.3 µm. Mass median aerodynamic diameter (MMAD) is a common measure of central tendency of a particle size distribution; it is the aerodynamic particle size of which half of the mass of the aerosol is in

smaller particles and half is in larger particles. Typical reported values of MMAD for welding fume are between 0.50 and 0.60 µm for shielded metal arc welding (SMAW) on mild steel and 0.20 to 0.30 µm for gas metal arc welding (GMAW) on mild steel (Hewett, 1995b, Isaxon et al., 2009, Antonini et al., 2011, Hewett, 1995a). Size distributions of flux-cored arc welding (FCAW) welding are reported less frequently, but MMADs in the range of 0.3-0.4 µm have been reported (Taube, 2013).

The aerodynamic size of inhaled particles largely determines the depth to which they can pass into the airways before deposition. The narrowing and branching of the airways from the nose and mouth down to microscopic alveoli distributes the particles throughout the respiratory tract according to their aerodynamic size (Carvalho et al., 2011). Impaction with airway walls, gravitational settling, and diffusion each act on particles according to their size; the three mechanisms together effectively filter inhaled particles as they pass through the airways so that smaller particles tend to reach farther.

The site of deposition is important because the eventual fate of a particle differs according to the region of the respiratory tract in which it comes to rest. Most inhaled foreign material is removed before it can be absorbed into the blood. Only Mn-containing particles that are deposited in the alveolar region are likely to contribute Mn for uptake directly from the respiratory system into the blood. Particles are continuously cleared from the respiratory tract by four mechanisms, the presence and relative importance of which vary by region. Removal by mechanical means, such as nose blowing, is possible only for particles trapped in the nasal region. Transport to the pharynx via the mucociliary escalator, a layer of mucous continuously carried up the walls of the airways by a layer of underlying cilia, and subsequent swallowing, is rapid for particles deposited in the trachea, bronchi, and bronchioles, but is not a feature of the

alveolar region (International Commission on Radiological Protection, 1994a). Mn in the GI tract is subject to strict homeostatic mechanisms that regulate absorption; excess is quickly cleared through biliary excretion (Aschner et al., 2005). Thus, Mn in particles that are inhaled and subsequently ingested is likely to have significantly less impact on blood Mn content than would Mn in particles that remain in the lungs. Transport into lymph nodes can take place from all regions, though rates are very low (International Commission on Radiological Protection, 1994a). While absorption into the bloodstream is also possible from other regions, it is only of real importance in the alveoli, because the alveoli alone lack the rapid transport to the GI tract or out of the body that dominate clearance in other regions (Oberdorster, 1988). Therefore, it is mostly the smallest inhaled particles that contribute Mn to the blood.

The inside walls of the alveoli are coated with a fluid that regulates moisture and protects the epithelium (Hatch, 1992). The precise mechanism by which Mn in the alveoli passes into the bloodstream is not well-understood, but it is clear that it must first dissolve from the particles in which it is contained. Though microscopic, the particles are far too large to pass into the blood by the same mechanisms that move single molecules of O_2 and CO_2. The solubility of the inhaled particles in the lung lining fluid would determine the availability of the particles' constituents for uptake into the bloodstream. Hatch's solution is a simulated lung lining fluid based on reports by Gary Hatch of the constituents of that fluid in humans (Hatch, 1992). Berlinger, et al. used Hatch's solution to estimate the solubility in the alveoli of SMAW, GMAW, and GTAW fume for up to 24 hours and found the solubility to vary between methods (2008). Ellingsen, et al. used the same method to assess fume from SMAW and GMAW and found the average solubility of Mn in Hatch's solution to be 13.8% (Ellingsen et al.)

While it has been shown that metals from welding fume remain in the lungs for significant lengths of time, it is unclear exactly where in the lungs they are held. Antonini et al, (2010) found that 53.2% of Mn from GMAW welding fume and 32.7% of Mn from SMAW welding fume remained in the lungs of rats 35 days after intratracheal instillation of welding fume. Similarly, 50% of iron from welding fume deposited in rat lungs remained at approximately 35 days (Kalliomaki et al., 1983). However, it is unknown from those reports if the particles are floating freely in lung fluid or are trapped within macrophages, epithelial cells, or the interstitial space. Besides absorption into the blood, the other significant routes of clearance for material in the alveolar region are through alveolar macrophages, immune cells which engulf and digest or remove foreign particles, and by transport through epithelial cells into the interstitial space and, from there, to the lymph system (Ferin, 1994). Semmler-Behnke, et al. found that three days post-exposure, only 5-10% of 17-20 nm iridium particles recovered from rat lungs were free, rather than contained within a macrophage or epithelial cell (Semmler-Behnke et al., 2007). While the lung response to iridium particles and welding fume cannot be assumed to be the same, this does give an idea of the speed with which the lungs may be able to sequester foreign material. However, there is a limit to the amount of material a macrophage can ingest, and a finite number of macrophages present at any moment in the lungs (Cannon, 1992). It is, therefore, worth considering that the number of ultrafine particles inhaled by a welder may overwhelm the capacity of the macrophages, leaving some fraction of the inhaled particles in the fluid lining the walls of the alveoli.

It is likely that the unclear relationship between exposure to airborne Mn and blood Mn is due, in part, to the fact that only a fraction of Mn contained in welding fume particles is rapidly absorbed into the blood. This paper describes an attempt to improve the estimate of welders'

systemic dose of inhaled Mn by incorporating particle size and solubility into exposure measurements. Here, we measured the particle size distributions and solubility in simulated alveolar lining fluid of fume generated by the five welding methods employed most by our study subjects. While welding fume particle size distributions have been widely described, and solubility in alveolar lining fluid has been the subject of recent studies, neither has been reported for all of the welding methods of interest. Fume from five methods of welding was examined separately because each of the methods is unique from the others in the combination of characteristics known to influence particle size, chemical composition, or both. SMAW, also known as manual metal arc welding or stick welding, uses consumable metal electrode rods coated in flux, which provides a microclimate in which the new weld is protected from oxidation. Volatilization of the flux material introduces elements not found in non-flux methods, such as K, Na, F, and S, into the fume particles (Berlinger et al., 2011). GMAW (formerly referred to as metal inert gas, or MIG, welding) uses a continuously-fed consumable wire. Instead of the flux used in SMAW, it employs a steady stream of gas, typically a mixture of argon and carbon dioxide, to envelop and protect the weld as it is created. Two methods of FCAW were tested; both use continuously-fed consumable wire that contains flux in its core. One, referred to as inner shield (here, abbreviated FCAW-IS) uses no shielding gas, while the other, dual shield (here, FCAW-DS) uses a stream of shielding gas similar to that used in GMAW, and is the only method of the five that uses both flux and shielding gas. The fifth method tested was gas tungsten arc welding (GTAW, formerly called tungsten inert gas, or TIG, welding). GTAW uses a non-consumable electrode, a shielding gas, and thin rods of a separate filler metal. Analysis of personal air samples collected for exposure assessment in the larger Mn

Biomarker project have found average Mn content for fume from each of the methods between 2.0% by weight (FCAW-IS) and 4.2% (FCAW-DS).

Methods

Fume was generated by student welders in ventilated booths in the welding shop of a technical college in the Seattle, Wash. area. All welding was done on mild steel.

Particle size distributions

Size-fractionated fume samples were collected with a 10-stage micro-orifice, uniform-deposit impactor (MOUDI) (MSP corp., model 110). The instrument separates particles aerodynamically and collects them on substrates that can be analyzed gravimetrically or otherwise. Each substrate collects aerodynamically-smaller particles than the substrate in the previous stage. Nominal cut-sizes, where collection efficiency is 50%, are 10, 5.6, 3.2, 1.8, 1.0, 0.56, 0.32, 0.18, 0.10, 0.056 µm. For example, stage 2, with a cut-size of 5.6 µm, is designed to collect particles with aerodynamic diameters of 5.6 µm to 10 µm (the cut-size of stage 1). Though stage size ranges are nominal limits on particle size, collection efficiencies of the MOUDI stages have been shown to provide separation near the nominal values (MSP Corporation, 2006). PTFE filters, 37mm, 2.0 µm pore size, (PALL, Inc., Zefluor filter) were used as substrates. The after filter, on which particles that pass the final stage collect, was a 37 mm, 2.0 µm pore size, Teflon filter (PALL, Inc., Teflo filter). The impactor was disassembled and cleaned before each sample was collected. At lower stages, the nozzle plates have orifices small enough that they can be clogged by particulate matter. Nozzle plates were inspected visually and cleaned with isopropanol and compressed air. Filter holders, which clamp the collection substrates in place, were also cleaned between each sample.

Samples were collected from approximately the same height as the welder's breathing zone. The MOUDI inlet was fitted with 30" of ¼" ID polyethylene tubing, the end of which was suspended with wire near the welder's head to allow the instrument itself to remain out of the work area. The potential particle loss due to the additional inlet tubing was calculated before sampling. Predicted transport loss was noticeable in the extreme ends of the size range where the smallest particles are drawn toward tubing walls by Brownian motion and larger particles are subject to inertial deposition if bends in the tube are too great and to settling if transport time is sufficiently long. It was determined that the tubing would cause negligible loss of particles in the size range of 0.01 to 4 µm in diameter. Calculations predicted approximately 20% loss for particles of 0.001 µm diameter and greater than 20% loss for particles exceeding 10 µm in diameter. The prescribed flow rate of 30 L/min was set before each run and tested again afterward.

Filters used as impactor substrates or after filters were weighed before and after sampling on a microbalance (Mettler-Toledo Inc., model UMT2). Filters were allowed to equilibrate in a temperature and humidity-controlled weighing chamber for a minimum of one week before either pre or post-sampling weighing. Filters were transported between the weighing chamber and the sampling site in labelled petri dishes.

The fraction of total sample mass captured in each stage was calculated and the cumulative mass fraction, i.e. the sum of the mass collected on a given stage's substrate and on all of the stages collecting smaller particles, were calculated. Cumulative mass fractions were then converted into the corresponding probit values for the standard normal distribution. A graph of log-transformed cut-size on these probit values yields a straight line if the data are log-normally distributed. This type of graph allows for simple calculation of the mass median

aerodynamic diameter and geometric standard deviation by exponentiation of the intercept and slope, respectively.

Deposition estimation

Fractional deposition was estimated using a model of respiratory deposition published by the International Commission on Radiological Protection (ICRP) (1994b). The model describes the mass fraction of an aerosol of given particle size that can be expected to deposit in each region of the respiratory tract. Input parameters include anthropometric characteristics and characteristics of the aerosol, among other factors. Published with the model are representative model outputs based on common input parameters. For example, values are available for expected deposition in the airways of adult nose-breathers engaged in light exercise or in children at rest. Because the particle diameters for which the model estimates deposition are not the same as the impactor stage ranges, the cumulative distribution graphs described above were used to interpolate mass fractions of each sample estimated to be in each ICRP size range. Those mass fractions were multiplied by the pre-calculated fractional deposition values for adult Caucasian males who are nose-breathers and engaged in light exercise, listed in Annexe F of the ICRP publication (James et al., 1994). The ICRP model describes the deposition expected in five regions, divided into seven fractions. The five regions are (1) the anterior nasal passages, (2) the posterior nasal passages, pharynx, and larynx, (3) the bronchi, (4) the bronchioles, and (5) the alveoli and surrounding interstitium. The model further divides the fractions deposited into the bronchi and bronchioles into those expected to clear by fast and slow mechanisms. Because the purpose of this project is not to model the clearance of inhaled particles, the fast and slow

clearance fractions for bronchi and bronchioles were combined into a single fraction for each region.

Solubility

Samples of fume generated by the five welding methods above were also collected on 37 mm, 0.8 µm pore size mixed-cellulose ester (MCE) membrane filters for use in solubility tests (SKC, Inc., part no. 225-1939). Solubility tests were not performed on size-fractionated samples because, while primary fume particles differ in chemical composition, aggregation of those diverse particles tends to create agglomerates that do not (Taube, 2013). Filters were housed in two-piece, closed-face, styrene cassettes and connected to personal sampling pumps calibrated to 2.0 L/min. Filters were suspended at the same height as the breathing zone of the welder, as near the welder as possible without disrupting the welding. All filters of a given welding type were not necessarily collected at the same time or from the same welder.

Each filter was leached for a specified duration in 10 ml of Hatch's solution. Solution components were purchased from Sigma-Aldrich, Inc. and were of the highest purity available, i.e. bioreagent grade for organic compounds and reagent or analytical grade for inorganic salts. The solution was prepared as described by Berlinger in one batch from which all 10 ml aliquots were drawn. Deionized water was prepared with a Barnstead EASYpure II purification system.

Leaching was done in the filter cup of a PALL Macrosep Advanced Centrifugal Device in an incubator at 37 C. The centrifugal filtering device consists of a 50 ml polypropylene centrifuge tube and a removable 25 ml cup with a 10 kDa pore-size filter. Four durations of leaching were tested: 1, 24, 48, and 96 hours. The 48-hour tests were done in triplicate to assess variability. To summarize, at the beginning of solubility testing, each MCE filter was loaded into

the top cup of a centrifuge filter device filled with 10 ml Hatch's solution; for each of five types of welding, six samples were begun, one to be processed at 1 hour, one at 24 hours, three at 48 hours, and one at 96 hours. At its specified time each filter was removed from the incubator and centrifuged at 3850 x g for 140 minutes. After centrifuging, the filter cup was removed and the tube, now containing only filtrate, was recapped. The MCE filter was removed and placed in a separate 50 ml polypropylene tube. The section of the centrifuge filter cup below the 10 ml mark, including both the polyethersulfone filter and its polypropylene housing, was cut with a hot knife into pieces small enough that all pieces would fit into the 50 ml tube with the MCE filter and sit below the 25 ml mark.

Samples were analyzed by inductively-coupled plasma mass spectrometry on an Agilent 7500-CE mass spectrometer. Preparation of processed samples for analysis was as follows. A 4.5 ml aliquot of each 10 ml filtrate sample was taken immediately after vortexing and digested by addition of 1 ml of concentrated HCl. Filter piece samples were prepared for analysis by a several step process of microwave-assisted acid digestion. Initially, 5 ml concentrated HCl and sufficient DI water to bring the volume to 20 ml was added to each filter piece sample. Subsequent microwave digestion did not fully dissolve the pieces, and two sequences, each consisting of the addition of 5 ml of concentrated HNO_3 and microwaving, were required to produce clear solutions.

Recovery of Mn was tested by adding known amounts of Mn to unexposed MCE filters in Hatch's solution and preparing and analyzing them by the procedure described, with the exception of incubation. Mn in both very insoluble MnO_2 and highly soluble $MnCl_2$ were used, separately, to test recovery, as Mn is present in welding fume in a variety of compounds.

Results

Particle size distributions

Sixteen particle size distribution samples were collected, three for each of the five types of welding and a fourth for FCAW-IS. A large fraction (10/16) of the after filters was found, upon disassembly of the impactor, to have torn. Gravimetric analysis was possible for the after filter for one sample from each of SMAW, GTAW, FCAW-IS, and FCAW-DS, and two of the GTAW samples. None of the collection substrates for stages above the after filter were damaged. Of the after filters that remained intact, each accounted for between 0.8% and 1.1% of the total sample mass, except for the two surviving GTAW after filters, which held 6.1% and 6.9% of their respective samples' masses. For consistency, analysis was performed as if all samples were missing data from the after filter. That is, mass fractions were calculated as though the smallest particles in the aerosol were 0.056 µm in aerodynamic diameter. To test the effect of excluding the after filters from analysis, MMADs and GSDs were calculated both with and without after filter data for those samples for which the after filter could be post weighed. Results of that comparison are presented in table 1.

Table 1. Comparison of calculated particle size distribution parameters with and without data for after filters. Includes the six samples for which the after filter survived sampling.

	MMAD (µm) (GSD)		% change in parameter after exclusion	
sample ID	**including after filter**	**excluding after filter**	**MMAD (µm)**	**GSD**
SMAW 2	1.40 (4.21)	1.44 (4.11)	3	-2
GMAW 1	1.06 (3.72)	1.13 (3.51)	7	-6
FCAW-IS 2	1.02 (3.55)	1.06 (3.45)	4	-3
FCAW-DS 1	0.79 (3.36)	0.79 (3.4)	0	1
GTAW 2	0.67 (5.39)	0.85 (4.55)	28	-15
GTAW 3	0.98 (8.71)	1.16 (8.21)	19	-6

Nearly all samples showed some tendency toward a bimodal particle size mass distribution, as is evident in graphs of log-transformed cut-size against probit value of the cumulative mass fraction (figure 1).

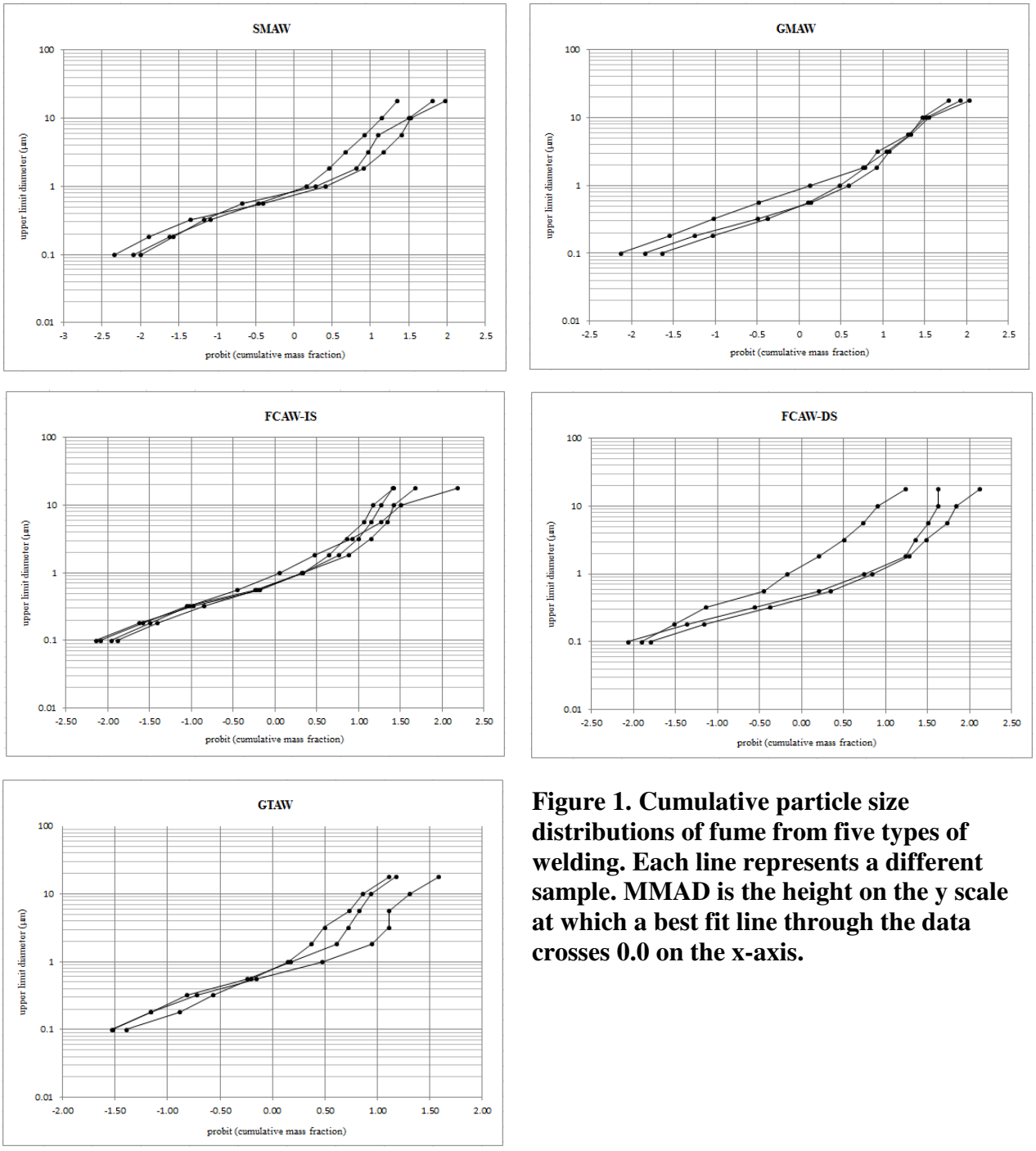

Figure 1. Cumulative particle size distributions of fume from five types of welding. Each line represents a different sample. MMAD is the height on the y scale at which a best fit line through the data crosses 0.0 on the x-axis.

Whereas a log-normally distributed sample would generate a straight line on such a graph, samples from all five measured methods of welding more closely approximated two straight lines of different slope, with a finer segment encompassing approximately particles ≤1 µm in aerodynamic diameter and a coarser segment made up of particles larger than 1 µm. Only a single FCAW-DS sample did not appear to be bimodal.

Size distribution parameters calculated for full samples (without after filters) are summarized in table 2. One-way ANOVA did not justify a claim that mass median aerodynamic diameters calculated from the entire size range differed according to welding type (P = 0.58).

Table 2. Characteristics of welding fume particle size distributions

		MMAD (µm)	GSD
	n	mean (sd)	mean (sd)
SMAW	3	1.25 (0.17)	3.55 (0.56)
GMAW	3	0.88 (0.22)	3.96 (0.49)
FCAW-IS	4	1.12 (0.05)	3.77 (0.40)
FCAW-DS	3	1.04 (0.60)	3.95 (0.88)
GTAW	3	1.06 (0.18)	6.21 (1.85)

Table 3 summarizes the same parameters calculated for the two apparent ranges of particle sizes.

Table 3. Characteristics of welding fume particle size distributions

		segment ≤ 1 µm		segment > 1 µm		fraction of sample mass in particles ≤ 1 µm
		MMAD (µm)	GSD	MMAD (µm)	GSD	
	n	mean (sd)	mean (sd)	mean (sd)	mean (sd)	mean (sd)
SMAW	3	0.62 (0.12)	2.49 (0.49)	2.95 (1.3)	4.67 (0.03)	0.61 (0.05)
GMAW	3	0.38 (0.1)	2.16 (0.15)	2.73 (0.99)	4.2 (1.2)	0.65 (0.09)
FCAW-IS	4	0.45 (0.01)	2.2 (0.19)	2.73 (1.02)	6.35 (2.67)	0.60 (0.05)
FCAW-DS	2*	0.35 (0.03)	1.94 (0.04)	1.48 (0.26)	12.79 (10.32)	0.67 (0.05)
GTAW	3	0.36 (0.07)	2.7 (0.08)	4.81 (2.38)	9.24 (3.95)	0.60 (0.07)

* One FCAW-DS sample did not appear bimodal and was not included in segmented analysis.

Deposition estimation

The estimated percent of sample mass expected to deposit in the alveolar-interstitium region ranged from 4.8 to 8.2%, with an arithmetic mean of 5.7%. The largest percentage of deposition is expected to occur in the extrathoric regions, which together comprise the nasal passages, larynx, and pharynx. Table 4 summarizes the expected overall deposition by weld method. It should be noted that the deposition values will not necessarily agree with penetration values described by, for example, the American Conference of Government Industrial Hygienists (ACGIH), and regional fractions will not add up to 100 % because deposition refers to both penetration and retention. That is, the ICRP model takes into account the fact that some particles that reach, for example, the alveolar region remain entrained in the air and leave the alveoli in exhaled air.

Table 4. Estimated percent of total sample mass deposited in airway regions

		ET_1	ET_2	bronchi	bronchioles	alveolar-interstitium
SMAW	n=3	19.9 (0.8)	24.1 (0.9)	1.2 (0.0)	1.0 (0.0)	**5.6 (0.1)**
GMAW	n=3	19.1 (0.4)	23.1 (0.5)	1.2 (0.0)	1.0 (0.0)	**5.6 (0.2)**
FCAW-IS	n=4	19.2 (1.6)	23.3 (1.7)	1.2 (0.0)	1.0 (0.1)	**5.8 (0.4)**
FCAW-DS	n=3	17.3 (4.4)	21.1 (4.7)	1.1 (0.1)	1.2 (0.3)	**6.5 (1.7)**
GTAW	n=3	19.7 (1.1)	23.7 (1.2)	1.2 (0.0)	0.9 (0.0)	**5.2 (0.3)**
Overall	n=16	19.1 (2.0)	23.1 (2.2)	1.2 (0.1)	1.2 (0.1)	**5.7 (0.8)**

Abbreviations: ET_1 (extrathoracic 1) is the anterior nasal passages. ET_2 comprises the remaining extrathoracic airways: the posterior nasal passages, the pharynx, and the larynx.

Solubility

The percentage of Mn that dissolved in Hatch's solution from SMAW, FCAW-IS, and FCAW-DS fume did not show clear trends with relation to leaching duration. Each of these series varied little, and in no clear direction between time points. In fact, the lowest percentage

dissolved for each of these three series was at 96 hrs. The percentage of Mn dissolved from GMAW samples increased at each time point to a maximum of 3.0% at 96 hours.

The absolute amount of Mn in the undissolved fraction was lower for all GTAW samples than for other samples, a reflection of the relatively small amount of fume generated by the GTAW method. Two of the GTAW samples - one 48 hour and the 96 hour sample, had soluble Mn measurements below the reporting limit of 0.07 µg/4.5 ml sample aliquot. Calculation of the percentage of Mn dissolved for those two samples used the measured amounts, despite their being less than the reporting limit. The three remaining data points for the GTAW series, 1 hr., 24 hrs. and one of the 48 hr. samples, show the most dramatic trend with leaching duration, though in the direction of less Mn dissolving with longer leaching.

Filter blanks were assembled and transported with sampling filters to and from fume collection at the technical college. Six of these blank filters underwent the solubility test alongside the fume samples. One blank sample was removed from the incubator, processed, and analyzed with each leaching-duration group. Hatch-soluble Mn was below the reporting limit for all blank filters. Hatch-insoluble Mn ranged from below the limit of reporting of 0.1 µg/sample to 0.3 µg/sample. By comparison, insoluble Mn in the loaded fume samples ranged from 2.5 µg to 197 µg, with a median of 20.9 µg.

Pooled variance was calculated from the variance of each fume type's 48 hour samples. The pooled standard deviation of the 48 hour-leaching measurements was used to calculate 95% confidence intervals for the percentage of total Mn dissolved for all leaching durations. Error bars in the chart showing the percent of total Mn dissolved represent those confidence intervals (figure 2).

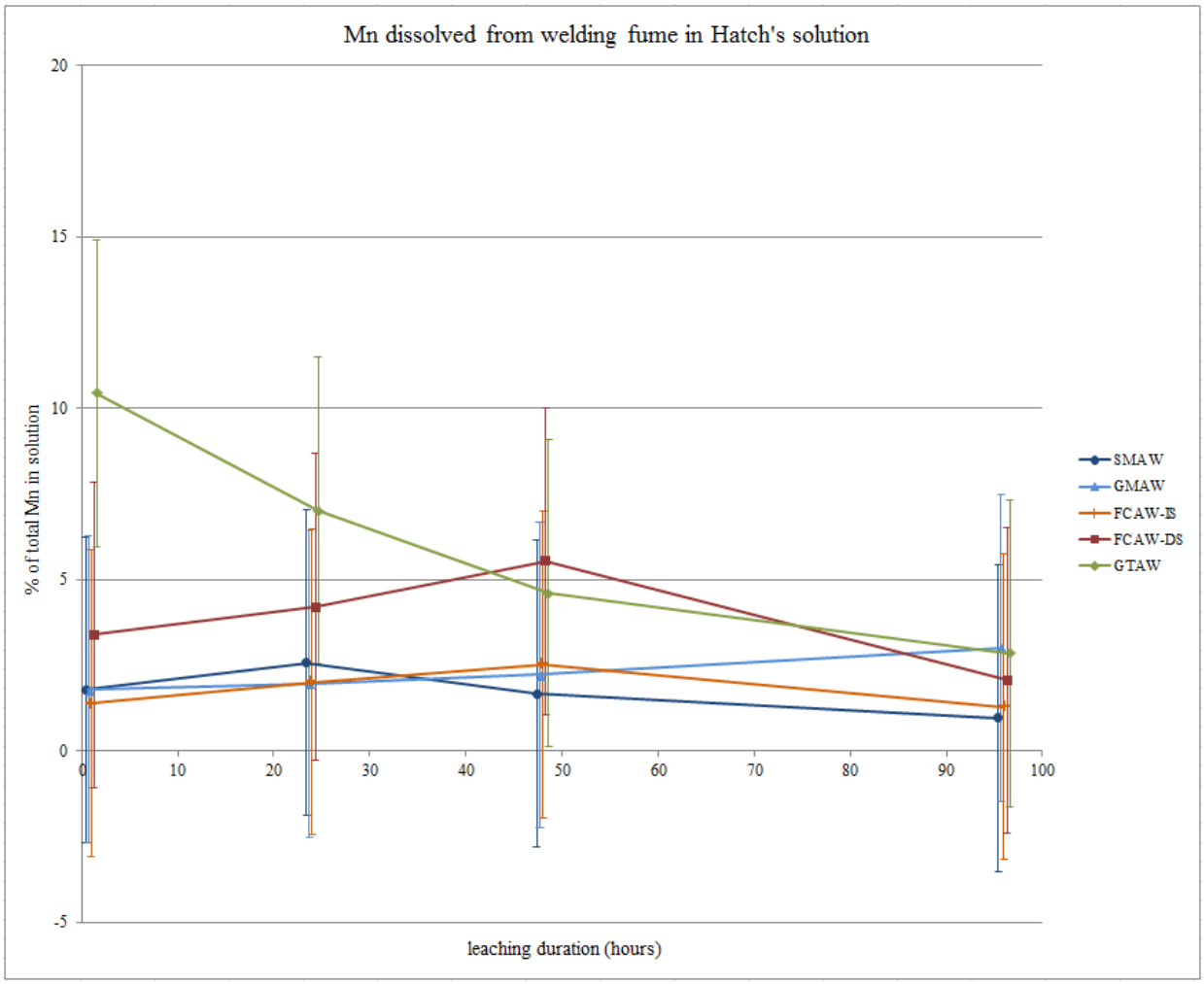

Figure 2. Percent of total sample Mn in Hatch's solution fraction of sample after leaching. Error bars represent 95 % confidence intervals based on the pooled variance of the 48 hour replicate samples. X-axis positions have been adjusted slightly to allow visual differentiation of error bars.

The estimated deposition and solubility were applied to Mn concentrations in personal air samples of subjects in the Mn Biomarker study to estimate the total Mn from a day's exposure expected to become available for uptake from the alveolar region into the blood. Intake was calculated based on the EPA-estimated 50th percentile ventilation rate for a 21-30 year old engaged in light exercise and an 8 hour time period. Using the average expected fractional deposition in the alveolar-interstitium region for each method (table 4) and an overall average

solubility for all samples of 3.2%, we calculated median and 90th percentile amounts of Mn expected to become available for absorption from a day's exposure to welding fume (table 5).

Table 5. Estimates of amount of Mn from inhaled welding fume that will become available for uptake into the blood from the alveoli.

	Mn inhaled in one day as measured in Mn Biomarker study (µg)		Mn expected to become available for uptake from one day of exposure (µg)	
	median	90th %	median	90th %
SMAW	226.2	547.6	0.4	1.0
GMAW	238.1	529.7	0.4	0.9
FCAW-IS	208.3	845.2	0.4	1.6
FCAW-DS	285.7	1089.2	0.6	2.3
GTAW	65.5	148.8	0.1	0.2

Discussion

Measured MMADs, if calculated as if the distributions are unimodal, are considerably higher than those typically reported in the literature. Explanations could include actual differences in the makeup of fume or sampling error. It is possible that the fume generated by the student welders is physically different than the fume produced by more experienced welders or automated processes more typical of welding fume studies. For example, fume formation in GMAW is affected by the mode of transfer of filler metal from the wire to the base metal, a characteristic that varies with voltage, amperage, wire feed rate, and technique. The transfer mode affects the quality and type of weld produced, and each mode has its applications. However, globular transfer, in which the largest droplets are transferred across the arc and the largest amount of spatter is introduced into the air, is easier to achieve than modes which generate finer droplets of metal and it can occur when attempting to achieve spray transfer. It may be that the skill level of the student welders resulted in fume with different particle size distribution than typical welding fume.

It is also possible that the welding fume generated for the study had typical physical characteristics, but that sampling methods skewed the results. One parameter of sampling that was atypical of cascade impactor use was the tubing on the inlet of the instrument. Calculations of expected particle loss predicted that inlet tubing would affect the collection of an aerosol of the size range of welding fume primarily by causing loss of particles larger than approximately 10 µm in diameter. Thus, particle loss is unlikely to explain the higher MMADs found in this study because the effect of the particle loss would be an underestimation of the MMAD. An overestimate of particle size measured by an impactor could also indicate that the air flow rate through the instrument was too high, causing particles to leave the airstream and impact upon earlier (larger) stages. However, the flow rate through the instrument, including the inlet tubing, was set with a rotameter to manufacturer-prescribed 30 L/min before sampling and tested after sampling. The flow rate was higher (6.7%) after sampling in only one case. It is also conceivable that the actual makeup of the fume was changed by the ¼" ID tubing. That is, pulling the fume through the tubing at nearly 16 m/s may have increased the aggregation of the particles by increasing their rate of collision.

Due to the similarity of the particle size distributions, deposition estimated with the ICRP model was very similar between different samples, both between and within different welding methods. A notable result of the deposition estimation is the small fraction of particles of any size that are expected to reach the alveolar region.

The solubility of the Mn observed was markedly lower than in previous reports. Berlinger et al., whose 2008 study provided the framework for our methods, found that 14% and 6.8% of Mn from GMAW and SMAW, respectively, had dissolved after 24 hours. The solubility of Mn at 24 hours in our tests of the same types of fume was 2.0% and 2.6%, respectively. There is

ample evidence that welding fume differs in physicochemical makeup as a function of the welding method used. The presence of flux in SMAW, FCAW-IS, and FCAW-DS introduces different compounds into the air surrounding the weld, and components of the flux varies between methods. Shielding gas affects the formation of fume particles and is only used in GMAW, FCAW-DS, and GTAW, of the methods we measured. As such, it is not unexpected to see different solubility between the different methods.

The overall low solubility could be a result of physical characteristics induced by any number of welding parameters, few of which could have been controlled in sampling, but some of which could, and should, have been recorded. A clear possible reason for the general difference in solubility between the two studies is that the Berlinger study used fume from stainless steel welding, while our welding was done on mild steel.

Regardless of previous reports of welding fume solubility, the flat response over time for fume from three of the welding methods is unexpected, as is the apparent time trend in solubility of GTAW fume. The lack of clear increase in dissolved Mn in fume from three of the methods could be interpreted as a reasonable measure of the general insolubility of welding fume. Possible reasons for the apparent decline in solubility of GTAW fume with longer leaching in Hatch's solution could include a change in the pH or redox potential of the solution over time due to microbial growth. Hatch's solution has a pH of 7.4, as normal lung fluid does. However, we failed to consider before the experiment that microbial growth could alter the pH of the solution. If the pH were increasing with time, Mn that had dissolved out of welding fume particles would become more likely to precipitate out in the form of highly-insoluble MnO_2. Had we measured the pH of the samples as they were removed from the incubator we would have a better idea of the likelihood of this scenario. While Hatch's solution was prepared according to

the description given by Berlinger et al., our experiments went as long as 96 hours, while Berlinger's tests ended at 24 hours. Perhaps our extended time period allowed for microbial growth not seen in the previous study.

Estimates of the amount of Mn inhaled by a subject in the Mn Biomarker study that should become available for uptake are several orders of magnitude lower than the adequate intake value for Mn ingestion provided by the National Academy of Sciences (2001). Our calculations estimate median amounts of Mn available for uptake of 0.1 to 0.4 μg, depending on welding method, whereas adequate intake for adults is 2.3 mg/day for males and 1.8 mg/day for females.

Conclusions

The lack of difference in particle size distributions between welding methods suggests that the type of welding that participants in our larger study were performing was not greatly affecting the fraction of inhaled fume that reached their lungs. The ICRP deposition model predicts that, on average, only about 5.7% of the mass of fume in our study will deposit in the alveoli. While the solubility tests are somewhat inconclusive, they suggest that only about 3.2% of the mass of Mn that does deposit in the alveolar region will dissolve from the fume and become available for uptake into the blood. Thus, only a very small fraction of Mn, approximately 0.2%, in welding fume should be available to enter the circulation from the respiratory tract.

Acknowledgements

The author would like to thank his committee for their support and guidance, as well as Michael Paulsen, Russell Dills, and Marissa Baker for their assistance in methods development.

Funding was provided by NIEHS grant # R01 ES017809.

References

ANTONINI, J. M., ROBERTS, J. R., CHAPMAN, R. S., SOUKUP, J. M., GHIO, A. J. & SRIRAM, K. 2010. Pulmonary toxicity and extrapulmonary tissue distribution of metals after repeated exposure to different welding fumes. *Inhal Toxicol,* 22**,** 805-16.

ANTONINI, J. M., ROBERTS, J. R., STONE, S., CHEN, B. T., SCHWEGLER-BERRY, D., CHAPMAN, R., ZEIDLER-ERDELY, P. C., ANDREWS, R. N. & FRAZER, D. G. 2011. Persistence of deposited metals in the lungs after stainless steel and mild steel welding fume inhalation in rats. *Arch Toxicol,* 85**,** 487-98.

APOSTOLI, P., LUCCHINI, R. & ALESSIO, L. 2000. Are current biomarkers suitable for the assessment of manganese exposure in individual workers? *Am J Ind Med,* 37**,** 283-90.

ASCHNER, J. L. & ASCHNER, M. 2005. Nutritional aspects of manganese homeostasis. *Mol Aspects Med,* 26**,** 353-62.

ASCHNER, M., ERIKSON, K. M. & DORMAN, D. C. 2005. Manganese dosimetry: species differences and implications for neurotoxicity. *Crit Rev Toxicol,* 35**,** 1-32.

ATSDR 2012. Toxicological Profile for Manganese. *In:* U.S. DEPARTMENT OF HEALTH AND HUMAN SERVICES (ed.) *Toxicological Profiles.* Atlanta, GA: Agency for Toxic Substances and Disease Registry.

BERLINGER, B., BENKER, N., WEINBRUCH, S., L'VOV, B., EBERT, M., KOCH, W., ELLINGSEN, D. G. & THOMASSEN, Y. 2011. Physicochemical characterisation of different welding aerosols. *Anal Bioanal Chem,* 399**,** 1773-80.

BERLINGER, B., ELLINGSEN, D. G., NARAY, M., ZARAY, G. & THOMASSEN, Y. 2008. A study of the bio-accessibility of welding fumes. *J Environ Monit,* 10**,** 1448-53.

BOWLER, R. M., ROELS, H. A., NAKAGAWA, S., DREZGIC, M., DIAMOND, E., PARK, R., KOLLER, W., BOWLER, R. P., MERGLER, D., BOUCHARD, M., SMITH, D., GWIAZDA, R. & DOTY, R. L. 2007. Dose-effect relationships between manganese exposure and neurological, neuropsychological and pulmonary function in confined space bridge welders. *Occup Environ Med,* 64**,** 167-77.

CANNON, G. J. S., J. A. 1992. The macrophage capacity for phagocytosis. *Journal of cell science,* 101**,** 907-13.

CARVALHO, T. C., PETERS, J. I. & WILLIAMS, R. O. R. 2011. Influence of particle size on regional lung deposition--what evidence is there? *Int J Pharm,* 406**,** 1-10.

ELLINGSEN, D. G., DUBEIKOVSKAYA, L., DAHL, K., CHASHCHIN, M., CHASHCHIN, V., ZIBAREV, E. & THOMASSEN, Y. 2006. Air exposure assessment and biological monitoring of manganese and other major welding fume components in welders. *J Environ Monit,* 8**,** 1078-86.

ELLINGSEN, D. G., KONSTANTINOV, R., BAST-PETTERSEN, R., MERKURJEVA, L., CHASHCHIN, M., THOMASSEN, Y. & CHASHCHIN, V. 2008. A neurobehavioral study of current and former welders exposed to manganese. *Neurotoxicology,* 29**,** 48-59.

ELLINGSEN, D. G., ZIBAREV, E., KUSRAEVA, Z., BERLINGER, B., CHASHCHIN, M., BAST-PETTERSEN, R., CHASHCHIN, V. & THOMASSEN, Y. 2013. The bioavailability of manganese in welders in relation to its solubility in welding fumes. *Environmental Science-Processes & Impacts,* 15**,** 357-365.

FERIN, J. 1994. Pulmonary retention and clearance of particles. *Toxicology letters,* 72**,** 1-3.

HATCH, G. E. 1992. Comparative Biochemistry of Airway Lining Fluid. *In:* PARENT, R. A. (ed.) *Treatise on Pulmonary Toxicology, Volume I: Comparative Biology of the Normal Lung.* 1st ed. Boca Raton, FL: CRC Press.

HEWETT, P. 1995a. Estimation of regional pulmonary deposition and exposure for fumes from SMAW and GMAW mild and stainless steel consumables. *Am Ind Hyg Assoc J,* 56**,** 136-42.

HEWETT, P. 1995b. The particle size distribution, density, and specific surface area of welding fumes from SMAW and GMAW mild and stainless steel consumables. *Am Ind Hyg Assoc J,* 56**,** 128-35.

INSTITUTE OF MEDICINE: PANEL ON MICRONUTRIENTS 2001. *Dietary Reference Intakes for Vitamin A, Vitamin K, Arsenic, Boron, Chromium, Copper, Iodine, Iron, Manganese, Molybdenum, Nickel, Silicon, Vanadium, and Zinc*, The National Academies Press.

INTERNATIONAL COMMISSION ON RADIOLOGICAL PROTECTION 1994a. Clearance model. *Annals of the ICRP* 24**,** 65-79.

INTERNATIONAL COMMISSION ON RADIOLOGICAL PROTECTION 1994b. Deposition model. *Annals of the ICRP* 24**,** 36-54.

ISAXON, C., PAGELS, J., GUDMUNDSSON, A., ASBACH, C., JOHN, A. C., KUHLBUSCH, T. A. J., KARLSSON, J. E., KAMMER, R., TINNERBERG, H., NIELSEN, J. & BOHGARD, M. 2009. Characteristics of welding fume aerosol investigated in three Swedish workshops. *J. Phys. Conf. Ser. Journal of Physics: Conference Series,* 151.

JAMES, A. C., ROY, M. & BIRCHALL, A. 1994. Annexe F. reference values for regional deposition. *Annals of the ICRP,* 24**,** 415-432.

KALLIOMAKI, P. L., JUNTTILA, M. L., KALLIOMAKI, K. K., LAKOMAA, E. L. & KIVELA, R. 1983. Comparison of the behavior of stainless and mild steel manual metal arc welding fumes in rat lung. *Scand J Work Environ Health,* 9**,** 176-80.

MSP CORPORATION 2006. *Model 100/110 MOUDI User Guide,* Shoreview, MN, MSP Corp.

OBERDORSTER, G. 1988. Lung Clearance of Inhaled Insoluble and Soluble Particles. *Journal of Aerosol Medicine,* 1**,** 289-330.

OPRYA, M., KIRO, S., WOROBIEC, A., HOREMANS, B., DARCHUK, L., NOVAKOVIC, V., ENNAN, A. & VAN GRIEKEN, R. 2012. Size distribution and chemical properties of welding fumes of inhalable particles. *AS Journal of Aerosol Science,* 45**,** 50-57.

ROELS, H., LAUWERYS, R., BUCHET, J. P., GENET, P., SARHAN, M. J., HANOTIAU, I., DE FAYS, M., BERNARD, A. & STANESCU, D. 1987. Epidemiological survey among workers exposed to manganese: effects on lung, central nervous system, and some biological indices. *Am J Ind Med,* 11**,** 307-27.

SEMMLER-BEHNKE, M., TAKENAKA, S., FERTSCH, S., WENK, A., SEITZ, J., MAYER, P., OBERDORSTER, G. & KREYLING, W. G. 2007. Efficient elimination of inhaled

nanoparticles from the alveolar region: evidence for interstitial uptake and subsequent reentrainment onto airways epithelium. *Environ Health Perspect,* 115**,** 728-33.
SJOGREN, B., IREGREN, A., FRECH, W., HAGMAN, M., JOHANSSON, L., TESARZ, M. & WENNBERG, A. 1996. Effects on the nervous system among welders exposed to aluminium and manganese. *Occup Environ Med,* 53**,** 32-40.
TAUBE, F. 2013. Manganese in occupational arc welding fumes--aspects on physiochemical properties, with focus on solubility. *Ann Occup Hyg,* 57**,** 6-25.
VISHNYAKOV, V. I., KIRO, S. A. & ENNAN, A. A. 2013. Formation of primary particles in welding fume. *Journal of Aerosol Science,* 58**,** 9-16.